

# Effect of Alloying Elements on Corrosion, Microstructure and Mechanical Properties for Casted Free-Nickel Duplex Stainless Steels

Ragaie Rashad, Amer E. Amer, Ahmed Y. Shash and Hany Shendy

**Abstract** Free nickel Duplex stainless steels containing two different levels of 6–13 wt% manganese contents have been studied and analysed. The alloys, made up of appropriate mixtures of the alloying elements, Ferro-alloys and Ferro-alloys bearing nitrogen were melted in an induction furnace under nitrogen pressure. Even though the resistance to the pitting attack was controlled and enhanced by the nitrogen addition as well as, chromium, molybdenum contents. Also, the cast experimental alloy that contained high manganese was found to offer some advantages over the 2205-type duplex stainless steel in combination of mechanical properties and corrosion resistance. The microstructure development due to increasing manganese contents from 6 to 13 wt% revealed the decrease of the ferrite volume fraction from 82 to 75 %, respectively. Mechanical testing results showed that the free nickel alloys containing 0.14–0.23 wt% carbon with manganese contents ranging from 6.44 to 13.45 wt% have moderate mechanical properties whereas U.T.S. ranging from (691–815) MPa, Y.S. (585–738) MPa, elongation (19–21 %), and a corrosion rate of 0.044–6.0 mm/year, respectively. Manganese is

---

Ragaie Rashad: on Leave from Cairo University

---

R. Rashad  
Department of Mechanical Engineering, British University in Egypt,  
11837 P.O. Box 43, Cairo, Egypt  
e-mail: Ragaie.Rashad@bue.edu.eg

A.E. Amer  
Mechanical Design and Production Engineering Department,  
Beni Suef University, Beni Suef, Egypt  
e-mail: aeid958@yahoo.com

A.Y. Shash (✉)  
Mechanical Design and Production Department, Faculty of Engineering,  
Cairo University, Giza, Egypt  
e-mail: ahmed.shash@cu.edu.eg

H. Shendy  
The Egyptian Technical Military School, Cairo, Egypt  
e-mail: shendy1969@yahoo.com

therefore an effective element of duplex microstructures. As an economical development, it is concluded that manganese is a useful replacement element for nickel in duplex alloys, but further work is required before the present alloys, or variations of them, could be commercially viable.

**Keywords** Free-Nickel duplex stainless steels • Corrosion resistance • Pitting attack • Microstructure development

## 1 Introduction

The industrial use of duplex stainless steel is rapidly increasing due to the combined advantages of better mechanical and corrosion properties [1–5]. Since the development of first-generation duplex stainless steels in the 1930s, considerable research efforts have been conducted to improve both mechanical and corrosion properties, particularly by controlling alloying elements, such as N, Cr, and Mo [3, 6–16]. Charles [4], for example, reported that the addition of Cr and/or Mo improved the resistance to pitting corrosion and stress corrosion cracking of duplex stainless steels. He further proposed that the addition of such elements needs to be done with caution since they can promote detrimental sigma phases at elevated temperatures [4]. Despite the extensive research works on the mechanical and corrosion behavior of duplex stainless steels, most of the researches have been conducted on the wrought products, and only a limited number of studies are available on the cast products of duplex stainless steels. Furthermore, Mn is often added to duplex stainless steel to increase the solubility of N to maximize the beneficial effect of N [17, 18]. According to the work of Gunn [19] and Kemp et al. [20] however, the effect of Mn on the microstructural evolution, as well as the mechanical and corrosion properties of duplex stainless steels have not been well established. The objective of the present study was therefore to examine the effect of Mn on the tensile and corrosion behaviour of free-nickel cast duplex stainless steels.

## 2 Experimental Procedures

The two experimentally proposed cast alloys of low and medium low carbon duplex stainless steel have been melted in a 10 kg laboratory induction furnace under nitrogen pressure around 8 bars and then cast in a metallic mould. The commercial duplex steels 2304 and 2205 grades were received in solution-annealed condition. The specimens were cut from plates and prepared for various property evaluations. The contents of alloying elements were determined, as shown in Table 1. The steels

**Table 1** Chemical composition of produced DSS

Alloying elements	Low carbon samples		DSS	
	Sample 1	Sample 2	2304	2205
C	0.14	0.232	0.02	0.02
Si	0.27	0.288	0.31	0.32
Mn	6.44	13.45	1.5	1.5
P	0.0056	0.05	0.04	0.04
S	0.031	0.017	0.03	0.03
Cr	24.8	23.33	22.9	21.9
Mo	1.76	1.79	0.4	3.0
Ni	0.19	0.2	4.7	5.7
N	0.21	0.199	–	–

were heat treated by homogenization at 1200 °C for 6 h to decrease chemical segregation by diffusion and to homogenize the overall microstructure.

Test samples were solution annealed at 1050 °C for 15 min and then water quenched to dissolve inter-metallic phases and restore mechanical properties and corrosion resistance to the as-cast duplex stainless steel. In order to reveal the microstructure, the specimens were polished mechanically and then electro etched. The set up for the electro etching was 12 V, 20 °C and the electrolyte was solution of 10 % oxalic acid +2 % nitric acid. In addition, in order to evaluate quantitatively the duplex phases, EDX analysis attached to SEM microscopy was carried out to the solution annealed specimens. Tensile and hardness test samples were prepared and tested to measure the mechanical properties of the different alloys. Eventually, the corrosion resistance of the two samples of free nickel duplex stainless steel was measured by polarization tests and immersion tests, and the results were compared with the commercial duplex stainless steels as DSS 2304 and 2205. All polarization studies were carried out in a single component cell with three electrode configurations. A silver/silver chloride electrode saturated with KCl was used as a reference electrode and a platinum sheet with surface area of 1 cm<sup>2</sup> as a counter electrode. The electrochemical experiments were carried out under computer control using the potentiostat AUTOLAB® PGSTATE 30, where the working electrode was a 1 cm<sup>2</sup> specimen immersed in a 3.5 % NaCl solution. The immersion test where the variation of the corrosion rate for Nitrogen alloyed steel samples was done by measuring the weight loss per unit area with time in 10 wt% absolute HCl solution at room temperature. Prior to the immersion, the samples were mechanically polished using 400, 500 and 600 emery papers and lubricated using distilled water. The samples were then cleansed with distilled water, dried in air, weighed for the original weight ( $W_o$ ) and then settled in the test solution. The corroded specimens were then removed from the solutions, cleansed with distilled water and dried, then the sample weight will be  $W_1$  and the weight loss is ( $W_o - W_1$ ). The corrosion attack was expressed in terms of weight loss per unit area (mg/cm<sup>2</sup>).

### 3 Results and Discussion

#### 3.1 Microstructural Evolution

The microstructural features of cast DSS are significantly influenced by the type and amount of alloying elements and the heat treatment applied. The solidification mode and the morphology of the primary delta ferrite phase as a leading phase, depends mainly on composition. Solidification can begin with primary ferrite or primary austenite.

In general, the microstructure of the as-cast alloys solidifies into the two different morphologies: acicular or globular, according to the amount of interstitial austenitic stabilization elements as Carbon, Manganese and Nitrogen.

According to XRD analysis, the microstructure solidified to a globular structure consisting of approximately 80 % volume fraction of ferrite and consequently, the remaining volume is austenite and some inter-metallic compounds or carbides, as shown in Fig. 1. The effect of homogenization shows a more or less homogenous structure with the disappearance of non-metallic inclusions which was found before

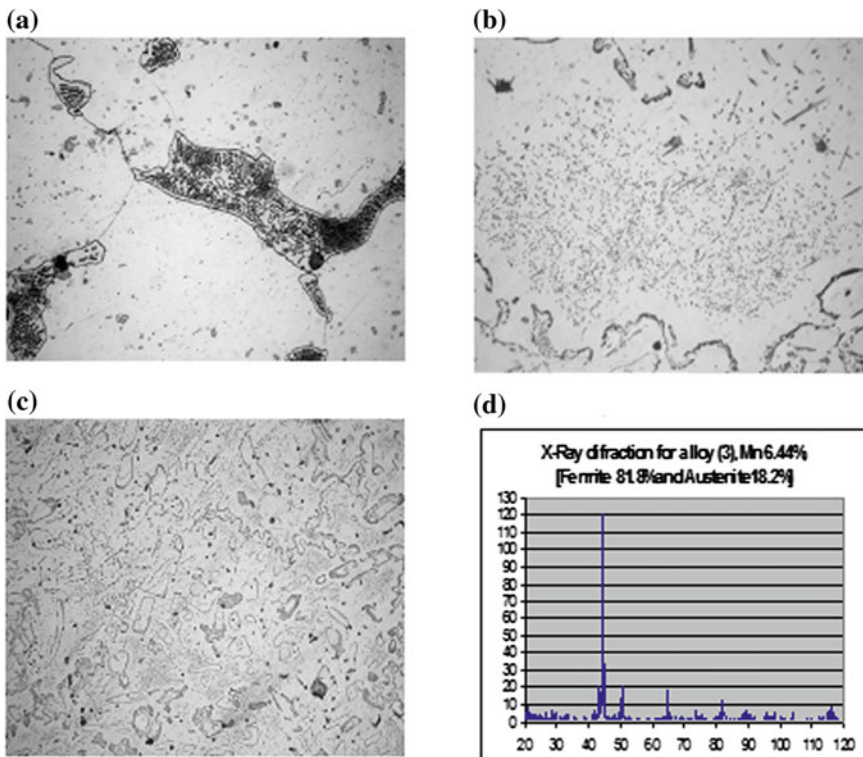


**Fig. 1** Microstructure of sample 1 containing 6.44 % Mn and 0.21 % N; **a** as cast, **b** homogenized, **c** solution annealed at 1050 °C, 30 min and **d** XRD analysis

as shown in Fig. 1a and b, respectively. Figure 1c illustrates the effect of the solution annealing treatment in dissolving the carbides and inter-metallic phases. On the other hand, the globular morphology is not modified even after solution annealing at 1050 °C.

As observed from Fig. 2, by increasing the manganese content, the amount of the austenite phase has a moderate increase and the structure had a ferrite volume structure of about 74 %, as investigated from the XRD analysis. Hence, improving in the tensile properties of that alloy was expected due to the increase of the amount of austenite phases compared with the previous commercial steel sample. Unfortunately, that improve in the mechanical properties was associated with a decrease in the corrosion resistance of this steel sample, as it will be discussed and mentioned later in the characterization and evaluation of corrosion properties. The role of homogenization annealing is still to modify the grains size to be more uniform and finer, decreasing the amount of non-metallic inclusion and chemical segregation by diffusion.

Table 2 shows the variation of ferrite volume fractions due to change of manganese contents.

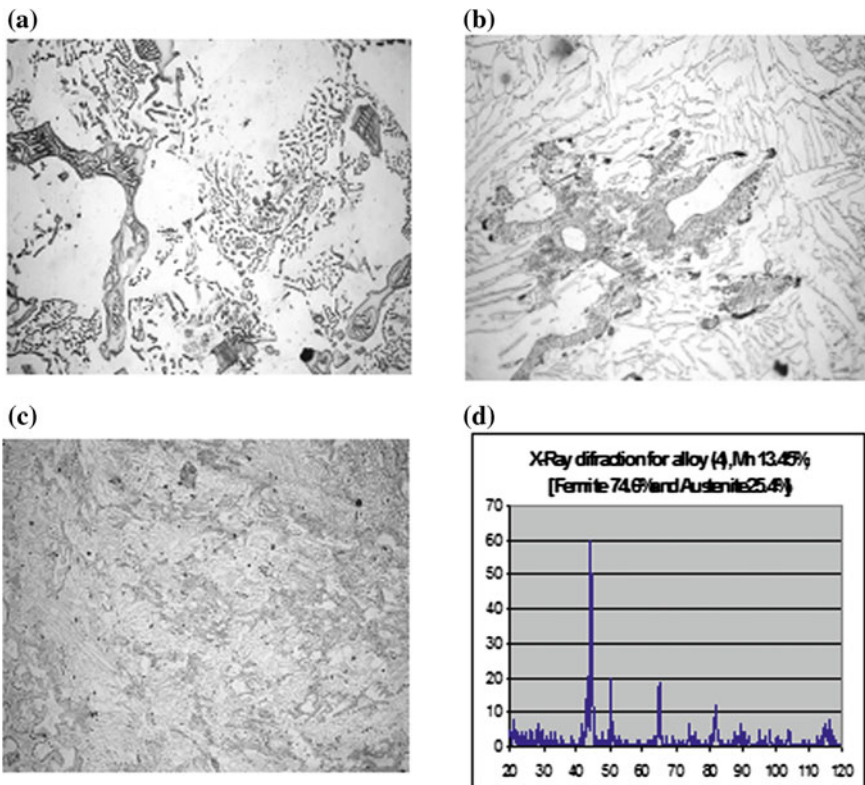


**Fig. 2** Microstructure of sample 2 containing 13.45 % Mn and 0.19 % N; **a** as cast, **b** homogenized, **c** solution annealed at 1050 °C, 30 min, and **d** XRD analysis

**Table 2** Characterization of phases by X-ray diffraction analysis

Sample no.	1	2
Manganese content	6.44 % Mn	13.45 % Mn
Volume fraction of ferrite	81.8 %	74.6 %

### 3.2 Mechanical Properties Evaluation

Mn is often added to stainless steels as an austenitic stabilizer for the partitioning effect of N [20]. In the present study, it was evident and demonstrated that different Mn contents significantly affect the tensile behaviour of the cast free nickel duplex stainless steel, as well as the corrosion behaviour. With increasing Mn content, the strength level was greatly increased from 691 to 815 MPa, while the tensile elongation was not notably reduced. Such a complex trend observed in tensile properties with varying Mn contents may be largely related to the microstructural evolution in the present alloy, including the volume fraction of each phase and the shape and size of the austenitic phase, both primary and secondary, along with an intrinsic solid solution hardening effect of Mn. Since, the austenitic phase is a harder phase than the ferritic phase, and the increase in the volume fraction of austenite would improve the strength level of cast duplex stainless steel, the remarkable increase in the yield strength value of the investigated alloy with increasing Mn content from 6.44 to 13.5 % was therefore attributed to the increase in the volume fraction of the austenite phase from 18.2 to 25.4 %, as well as the solid solution hardening effect of Mn as was evident in Fig. 3. The ultimate tensile strength value appeared to be related to the ductility which represents the capability of plastic deformation. The complex trend associated with the ultimate tensile strength values observed in Table 3 was therefore believed to be due to the intrinsic hardening effect of Mn and the change in tensile properties with Mn content in comparison to the commercial DSS 2304 and 2205. The decrease in the elongation with increasing Mn content appeared to be dependent on the change in the shape of the primary and secondary austenitic phase.

The one major advantage of duplex stainless steels is their high yield strength. For high Mn DSS, the yield strength is increased but the ductility and toughness are reduced. Both Ni-free DSS exhibit yield strengths of at least 550 to 750 MPa in combination with an elongation to fracture of at least 20 %.

### 3.3 Corrosion Resistance Measurement

Nitrogen increases the resistance to pitting corrosion, especially in combination with molybdenum.

**Fig. 3** Load-elongation curve for Sample 1 and 2 with 6.44 and 13.45 wt% Mn, respectively

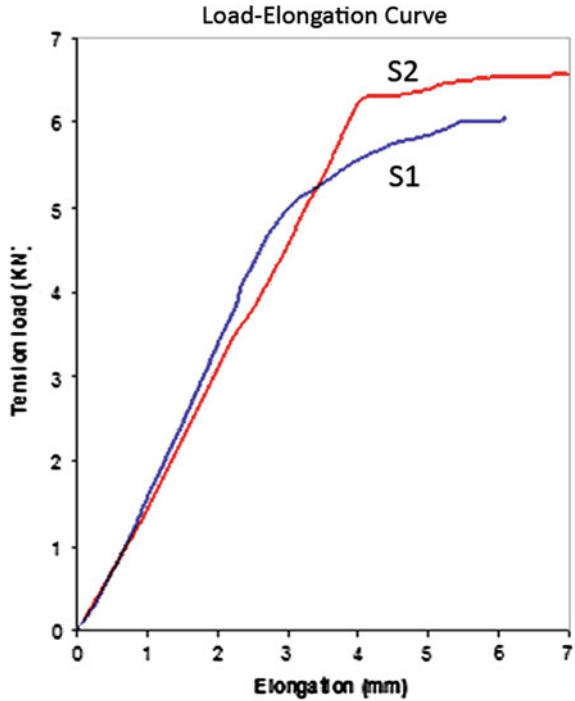


**Table 3** The results of mechanical properties of the experimental samples

Sample no.	U.T.S. (MPa)	Y.S. (MPa)	Elong. (%)	Impact energy j	Brinell hardness (BHN)
1	691	585	19	180	200
2	815	738	21	170	230
DSS 2304	663	480	40	180	190
DSS 2205	758	540	41	170	270

The Pitting Resistance Equivalent (PRE) was calculated according to the following equation [21]:

$$PRE = \%Cr + 3.3 \times \%Mo + 20 \times \%N$$

The pitting resistance results for samples 1 and 2 are illustrated in Table 4.

The polarizations resistance  $R_p$  was measured by scanning the potential in a range between  $\pm 15$  mV around the corrosion potential  $E_{corr}$  at 0.1 mV/s. From the current density versus potential plot the reciprocal of the slope of the curve  $dE/dI$  was determined at the corrosion potential in resistance units ( $\text{Ohm}/\text{cm}^2$ ).

**Table 4** PRE for samples 1 and 2

Sample no.	Sample 1	Sample 2	Duplex 2304
PRE	33.01	33.17	35

The corrosion current densities in  $\mu\text{A}/\text{cm}^2$  were calculated from the polarization resistance values using the Stern–Geary equation, [22]

$$I_{corr} = \frac{B_a \times B_c}{2.303(B_a + B_c)} \quad (1)$$

where the Tafel constants  $B_a$  and  $B_c$ , are the slopes of tangents drawn on the respective anodic and cathodic polarization plots in mV/decade. Subsequently, the corrosion rate ( $C_R$ ) was determined in mpy using the relationship:

$$C_R = \frac{0.13 \times I_{corr} \times eq.wt.}{\rho} \quad (2)$$

where  $\rho$  the density of the material ( $\text{g}/\text{cm}^3$ ) and  $I_{corr}$  the current density ( $\mu\text{A}/\text{cm}^2$ ).

The  $R_p$  is representative of the degree of protection of the passivation layer of the alloy surface. An increase in values of  $R_p$  improves the corrosion resistance of steel. The corrosion characteristics ( $R_p$ ,  $I_{corr}$ ,  $B_a$ ,  $B_c$ ,  $C_R$ ) were determined and the results summarized in Table 5. The values of  $R_p$  allow a comparison scale to be established. The highest polarization resistances were revealed by S.1 of  $2.94 \times 10^6$  Ohm/ $\text{cm}^2$ , while S.2 showed lower polarization resistances of  $1.21 \times 10^3$  Ohm/ $\text{cm}^2$ . Based on the estimated  $R_p$  values, it seems that the general corrosion behaviour of nitrogen–manganese stabilized austenitic steels is better than “conventional” steels of type 2304.

The Tafel slopes  $B_c$ ,  $B_a$  were determined by the fitting of a theoretical polarization curve to the experimental polarization curve plotted in the range of  $\pm 150$  mV versus Eoc. The corrosion current  $I_{corr}$  is representative of the degree of degradation of the alloy. An alloy with a tendency towards passivity will have a value of  $B_a$  greater than  $B_c$ , whereas an alloy that corrodes will have a  $B_a$  lower than  $B_c$ . It can be noticed from Table 5, that regarding to the Tafel slope results, it was found that steels DSS 2304 and S.2 reveal a tendency towards depassivity. For S.1,  $B_a$  is higher than  $B_c$  indicating to passivation ability.

**Table 5** Comparison of the electrochemical quantities measured and calculated for the various steels (37 °C)

Sample	$B_a$	$B_c$	$R_p$ , (Ohm)	$I_{corr}$ , ( $\mu\text{A}/\text{cm}^2$ )	$C_R$ , (mpy)
DSS 2304	0.021	0.038	1.58E4	3.67	0.98
S.1	0.039	0.027	2.94E6	0.15	0.044
S.2	0.007	0.068	1.21E3	22.5	6.0

$B_c$  and  $B_a$  tafel slopes, corrosion potential;  $R_p$  polarization resistance;  $I_{corr}$  corrosion current,  $C_R$  corrosion rate



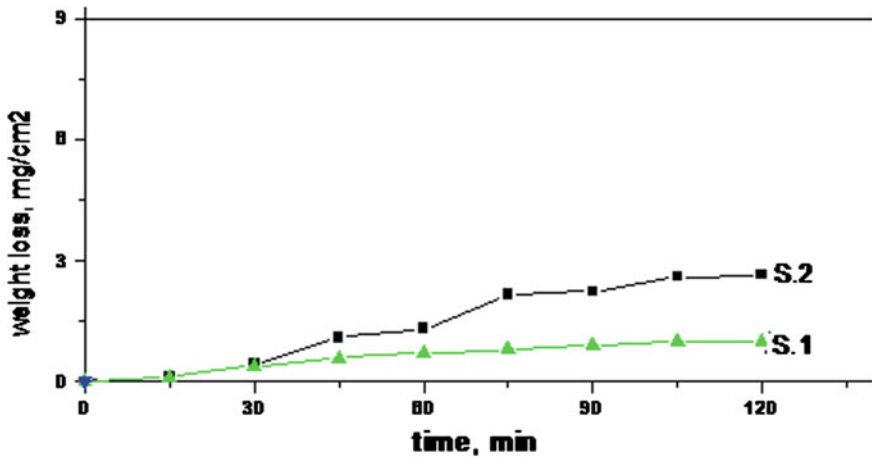


Fig. 4 Corrosion rate versus exposure time in 10 wt% HCl

Generally, the corrosion behavior of nitrogen–manganese stabilized austenitic steels S.1 is better than S.2.

The weight losses of Duplex Stainless Steel alloys in 10 %wt HCl have been determined as a function of the immersion time. The tested sample was immersed at room temperature in 10 %wt HCl for various immersion periods (0–120 min). The variation of the corroded weight (weight loss) with immersion time is shown in Fig. 4. It is obvious that the weight loss  $W_{\text{loss}}$  ( $\text{mg}/\text{cm}^2$ ) increased linearly with immersion time.

The resistance to pitting corrosion is associated with nonmetallic inclusions present in the alloys. Alloys S.1 and S.2 are more pitting resistance due to their low carbon content of 0.14 and 0.232 %, respectively. The data indicated that the annual corrosion rate of S.1 was the lowest due to probably its highest Mn content, i.e. the increase in Mn content of the alloys decreased the resistance to pitting corrosion. It can be concluded that the results of electrochemical polarization and immersion tests are coincident.

## 4 Conclusion

Two kinds of nickel-free duplex stainless steels have been developed in this scientific research work. These alloys can be characterized by their high strength and toughness, good corrosion resistance and low alloy element cost. In comparison with the commercial DSS with a similar  $\text{PRE}_N$ , the experimental DSS have a higher yield strength by roughly 100–200 MPa and a lower elongation to fracture of about 20 %. The increase in yield strength and ultimate tensile strength value of the investigated alloy with increasing Mn content from 6.44 to 13.5 % was therefore

attributed to the increase in the volume fraction of the austenite phase from 18.2 to 25.4 %, as well as the solid solution hardening effect of Mn. Microstructural investigations showed that such alloys have relatively stable austenite content at high temperatures. Due to the absence of nickel, the experimental DSS exhibit an excellent resistance to SCC in chloride solutions. Finally, these alloys can be cost-efficient because of the total absence of the expensive element nickel and therefore can find applications where high strength and moderate corrosive resistance are required.

**Acknowledgments** The authors would like to thank the late Prof. Dr.-Ing. Y. Shash the Head of the Mechanical Design and Production Department, Faculty of Engineering, Cairo University for his kind support and wise scientific advices. Thanks goes to Dr. A. Abd Elaal from Department of Metals Technology, Central Metallurgical Research and Development “CMRDI”, Helwan-Cairo Egypt for the corrosion tests.

## References

1. Huang J, Altstetter C (1995) Cracking of duplex stainless steel due to dissolved hydrogen. *Metall Mater Trans A* 26A:1079–1085
2. Davis J (1996) ASM specialty handbook stainless steels. ASM International, Materials Park, OH, pp 32
3. Solomon H, Devine T (1983) In: Lula RA (ed) Duplex stainless steels. ASM, Metals Park, OH, pp 693
4. Charles J (1994) In: Proceedings of the fourth international conference on duplex stainless steels, vol 1. Paper KI, Glasgow
5. Nicholls J (1994) In: Proceedings of the fourth international conference on duplex stainless steels, vol 1. Paper KIII, Glasgow
6. Son J, Kim S, Lee J, Choi B (2003) Effect of N addition on tensile and corrosion behaviors of CD4MCU cast duplex stainless steels. *Metall Mater Trans A* 34A:1617
7. Son J, Kim S, Lee J, Choi B (2002) Slow strain rate tensile behavior of CD4MCU cast duplex stainless steel with different nitrogen contents. *J Korean Inst Met Mater* 40:723
8. Park Y, Lee Z (2001) The effect of nitrogen and heat treatment on the microstructure and tensile properties of 25Cr–7Ni–1.5Mo–3W–xN duplex stainless steel castings. *Mater Sci Eng A* 297:78
9. Son J, Kim S, Lee J, Choi B (2003) Tensile and Corrosion Behaviors of As-solutionized CD4MCU Cast Duplex Stainless Steel with Different Nitrogen Contents. *J Korean Inst Met Mater* 40:949
10. Sakai J, Matsushima I, Kamemura Y, Tanimura M, Osuka T (1983) In: Lula RA (ed) Duplex stainless steels. ASM, Metals Park, OH, pp 211
11. Kim S, Paik K, Kim Y (1998) Effect of Mo substitution by W on high temperature embrittlement characteristics in duplex stainless steels. *Mater Sci Eng A* 247:67
12. Poznansky A, Nalbome C, Crawford J (1983) In: Lula RA (ed) Duplex stainless steels. ASM, Metals Park, OH, pp 431
13. Kim J, Park C, Kwon H (1999) *Bull Korean Inst Met Mater* 12:635
14. Guha P, Clark C (1983) In: Lula RA (ed) Duplex stainless steels. ASM, Metals Park, OH, pp 355
15. Okazaki Y, Miyahara K, Hosoi Y, Tanino M, Komatsu H (1989) Effect of alloying elements of  $\sigma$  phase formation in Fe-Cr-Mn alloys. *J Jpn Inst Met* 53:512

16. Speidel M (1991) In: Proceedings of the international conference on stainless steels, vol 1. ISIJ, Chiba, p 25
17. Nilsson J (1992) Superduplex stainless steels. *Mater Sci Technol* 8:685
18. Merello R, Botana F, Botella J, Matres M, Marcos M (2003) Influence of chemical composition on the pitting corrosion resistance of non-standard low-Ni high-Mn-N duplex stainless steels. *Corros Sci* 45:909
19. Gunn R (1997) Duplex stainless steel. Abington, Cambridge, p 15
20. Kemp AR, Dekker NW, Trincherro P (1995) Differences in inelastic properties of steel and composite beams. *J Constr Steel Res* 34:187–206
21. Gunn R (ed) (1997) Duplex stainless steels—microstructure, properties, and applications. Abington Publishing, Cambridge
22. Stern M, Geary A (1957) Electrochemical polarization: I. A theoretical analysis of the shape of polarization curves. *Electrochem J* 56–63